g Factor of Hydrogenlike $^{28}Si^{13+}$

S. Sturm,[1,2] A. Wagner,[1] B. Schabinger,[1,2] J. Zatorski,[1] Z. Harman,[1,3] W. Quint,[4] G. Werth,[2] C. H. Keitel,[1] and K. Blaum[1]

[1]*Max-Planck-Institut für Kernphysik, Saupfercheckweg 1, 69117 Heidelberg, Germany*
[2]*Institut für Physik, Johannes Gutenberg-Universität, 55099 Mainz, Germany*
[3]*ExtreMe Matter Institute EMMI, Planckstraße 1, 64291 Darmstadt, Germany*
[4]*GSI Helmholtzzentrum für Schwerionenforschung GmbH, Planckstraße 1, 64291 Darmstadt, Germany*

(Received 6 May 2011; published 7 July 2011)

We determined the experimental value of the g factor of the electron bound in hydrogenlike $^{28}Si^{13+}$ by using a single ion confined in a cylindrical Penning trap. From the ratio of the ion's cyclotron frequency and the induced spin flip frequency, we obtain $g = 1.995\,348\,958\,7(5)(3)(8)$. It is in excellent agreement with the state-of-the-art theoretical value of $1.995\,348\,958\,0(17)$, which includes QED contributions up to the two-loop level of the order of $(Z\alpha)^2$ and $(Z\alpha)^4$ and represents a stringent test of bound-state quantum electrodynamics calculations.

DOI: 10.1103/PhysRevLett.107.023002 PACS numbers: 31.30.js, 06.20.Jr, 12.20.−m, 37.10.Ty

Atomic physics has been a field of great importance for the development of quantum electrodynamics (QED) since its very beginning. Many crucial results, e.g., the Lamb shift, were related to the energy of atomic levels. The development of Penning trap experimental techniques has greatly improved the accuracy of measurements. Particularly noteworthy is the determination of the free-electron g factor [1]. Also measurements on the bound electron g factor [2,3] have been performed, thereby triggering a high tide of interest in that field [4–6]. The comparison between experimental and theoretical results of the g factor not only constitutes a very precise test of bound-state QED calculations but also has led to the accurate determination of some fundamental physical constants such as the electron mass [2,3].

These measurements were, however, restricted thus far to the regime of light elements such as C and O. An extension to heavier systems provides new insights into fundamental physics: As QED terms increase with high powers of the charge number Z, their contributions will be increasingly visible. Besides one-loop self-energy and vacuum polarization corrections, the contribution of two-loop diagrams shows up. Also, as the strength of the binding potential, characterized by the dimensionless quantity $Z\alpha$, with α being the fine-structure constant, increases, a more accurate description of QED effects in terms of this expansion parameter is called for. Ultimately, the regime will be reached where a nonperturbative treatment in terms of $Z\alpha$ is inevitable. Moreover, as the overlap of the electronic and nuclear wave functions increases, experimental g factors for heavier elements can provide new access to electromagnetic nuclear properties such as charge radii, deformation parameters, or polarizabilities. In all these investigations, it is highly informative if not only the charge number but at the same time the experimental accuracy can be increased.

In the present Letter, we present a new and precise experimental value of the g factor of the electron bound in the ground state of hydrogenlike $^{28}Si^{13+}$ representing the most stringent test of bound-state QED calculations to date. The experiment has been performed by using a single ion confined in a Penning trap. The setup has been described in detail in Refs. [7,8]. A triple Penning trap is located in a magnetic field B_0 of 3.76 T and is in thermal contact with a liquid helium bath. It consists of a stack of cylindrical electrodes of 7 mm inner diameter (Fig. 1). By applying the proper voltages to the electrodes, three potential minima in which the ion can be trapped are created. The first one, which we call a creation trap, serves for ionization of atoms released from a target after electron bombardment. Consecutive ionization by an electron beam of 4-keV energy for a couple of seconds creates ions of different elements and isotopes in a variety of charge states. The ion cloud is then transported to a second trap (precision trap) by adiabatic changes of the trap potentials. This trap consists of five electrodes in order to create a very harmonic trapping potential. Unwanted species are removed from the trap by selective excitation of their axial oscillation until only $^{28}Si^{13+}$ remains. Careful reduction of the trapping potential removes ions from the trap until only a single one is left. Its axial oscillation is brought into resonance with a tuned superconducting circuit with a quality factor of $Q = 950$ attached to an end-cap electrode. The circuit serves for resistive ion cooling to the ambient

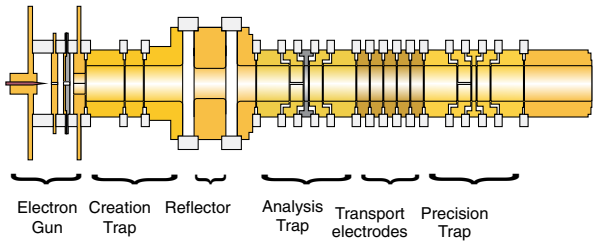

FIG. 1 (color online). Sketch of the triple Penning trap. For details, see the text.

temperature with a time constant of ~80 ms. The presence of the single ion is monitored by a minimum in the Fourier transform of the noise power across the tuned circuit. The low damping constant of the axial ion oscillation and the harmonic potential lead to a narrow and symmetric axial resonance of 1 Hz width at a frequency of 700 kHz. The single cooled ion is then transported to the third trap (analysis trap) separated from the precision trap by electrodes of 4.3 cm length. Similarly as in the precision trap it is monitored by its axial oscillation at 420 kHz. The center frequency can be determined to 20 mHz. A particular characteristic of the analysis trap is the central ring electrode consisting of ferromagnetic nickel. It distorts the homogeneous magnetic field of the trap in a bottlelike manner. The inhomogeneity is required to determine the spin direction of the bound electron through the "continuous Stern-Gerlach effect" [9]: The second term in a series expansion of the magnetic field $B = B_0 + B_2 z^2 + \cdots$ leads to a force $F = \mu \nabla B = 2\mu B_2 z$ acting on the magnetic moment μ of the electron. This force adds to or subtracts from the electric trapping force depending on the orientation of μ with respect to B_0 and changes the axial oscillation frequency. Because of the linear dependence of the magnetic force on z, the oscillation remains harmonic. For our parameters ($B_2 = 10$ mT/mm^2) the axial frequency difference for the two spin directions amounts to 240 mHz. In order to distinguish such a small frequency change upon an induced spin flip from frequency changes arising from fluctuating trapping potentials, extremely stable voltage sources are required [10]. A voltage change as low as 3 μV would mimic a spin flip. We use a source showing fluctuations below 1 μV in several minutes (stahl-electronics, UM1-14). This allows unambiguous detection of spin flips as shown in Fig. 2. After determination of the spin direction in the analysis trap, the ion is transferred back to the precision trap. Here the magnetic field is homogeneous apart from a small residual inhomogeneity of $B_2 = 0.6(1.4)$ μT/mm^2. In the precision trap the ion is irradiated by microwaves of frequency ν_{MW} near the Larmor frequency of the bound electron at $\nu_L \approx 105$ GHz. Simultaneously the eigenfrequencies of the ion's oscillation are measured: The axial frequency $\nu_z = 700$ kHz as described above, the perturbed cyclotron frequency $\nu_+ = 27$ MHz by coupling the cyclotron oscillation to the axial oscillation through a radio-frequency coupling field resulting in a split of the axial resonance ("double dip") [7,11], and the magnetron frequency $\nu_- = 9$ kHz similarly. From the three measured frequencies the ion's free cyclotron frequency $\nu_c = qB_0/(2\pi M)$ is determined via the Brown-Gabrielse invariance theorem $\nu_c^2 = \nu_+^2 + \nu_z^2 + \nu_-^2$ [12], which makes ν_c independent to trap misalignments to first order. Here q is the ion's charge state and M its mass. The determination of the oscillation frequencies and the attempts to induce a spin flip take approximately 90 s. Then the ion is transferred back to the analysis trap, and by measuring its axial frequency it is determined whether a spin flip in the precision trap has taken place or not. A successful detection of a spin flip is demonstrated in Fig. 2. The spin direction has changed after the ion has been irradiated by microwaves in the precision trap. This sequence is repeated many times at different microwave frequencies. The total time for a complete sequence including transfer and ion cooling takes about 1000 s. When the number of successful spin flips is recorded vs the microwave frequency, one obtains a resonance curve as shown in Fig. 3. Here the number of

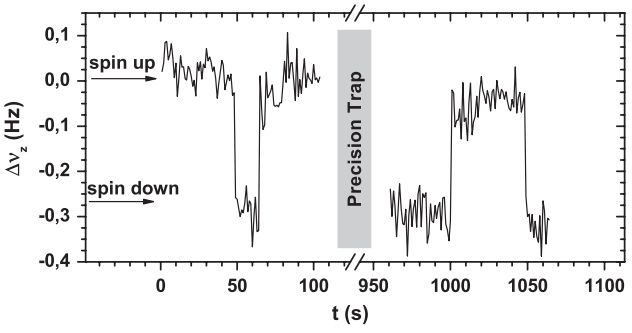

FIG. 2. Change in the axial ion's oscillation frequency upon induced spin flips in the analysis trap. The calculated frequency difference is 240 mHz in a total frequency of 420 kHz in fair agreement with the observation. Between the left and right periods, the ion was transported into the precision trap where a spin flip was successfully induced by irradiation with microwaves.

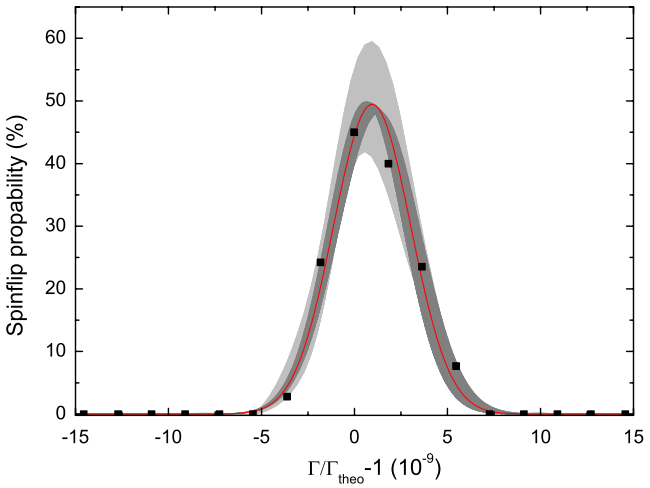

FIG. 3 (color online). Number of observed axial frequency jumps normalized to the total number of attempts to induce a spin flip. As the abscissa we plot the ratio $\Gamma = \nu_{\mathrm{MW}}/\nu_c$ of the simultaneously measured cyclotron frequency ν_c and the microwave frequency ν_{MW}. The data are fitted with a Gaussian by using the maximum-likelihood method, avoiding the need for data binning. The light gray area indicates the 68% prediction band for the measurement data distribution, while the dark gray area is the confidence band of the fit. The fractional statistical uncertainty of the resonance center of this single resonance is 4×10^{-10}.

spin flips is normalized to the total number of attempts to induce spin flips. Care has been taken to keep this number well below 50% by adjustment of the microwave power in order to avoid power broadening. From a maximum-likelihood fit to the data using a Gaussian line shape, we obtain the Larmor frequency $\nu_L = g\mu_B B_0$, where μ_B is the Bohr magneton. Since B_0 is determined through ν_c, we plot the ratio $\Gamma = \nu_{\mathrm{MW}}/\nu_c$ in Fig. 3 and denote the resonance center as Γ_0'.

We have taken six resonance lines at different microwave powers to make sure that no power-dependent line shift occurs. Each resonance line contains about 200 data points, and the recording took 2–3 days each. No systematic variation outside the statistical scatter is observed. Our result from the weighted average of the six resonances is $\Gamma_0' = 3912.866\,067(1)$ with a 1σ-fractional statistical uncertainty of 2.6×10^{-10}.

Systematic shifts of the measured frequencies may arise from different sources. Most important are image charges which the oscillating ion induces in the trap electrodes. Because of the dominant role of the perturbed cyclotron frequency in the determination of the magnetic field strength, we can neglect the effects on the axial and magnetron oscillation. The shift of the cyclotron frequency has been calculated by Van Dyck *et al.* [13] and Porto [14]. It amounts to $\delta\omega_c/\omega_c = (3Mc^2)/(2a^3B_0^2)$, where a is the trap radius. For our case of $M = 28$ u, $a = 3.5$ mm, and $B_0 = 3.76$ T we obtain a fractional shift of -6.87×10^{-10} with an estimated uncertainty 3.4×10^{-11}. We apply this downwards shift to our experimental value of the cyclotron frequency. Relativistic shifts $\delta\omega_c/\omega_c = kT/Mc^2$ amount to 6×10^{-13} and can be neglected as well as shifts from the residual magnetic field inhomogeneity. Our final experimental result is $\Gamma_0 = 3912.866\,064(1)$.

To derive the g factor from

$$g = 2\frac{\nu_L}{\nu_c}q(m_e/M) = 2\Gamma_0 q(m_e/M), \tag{1}$$

we take the electron mass as $5.485\,799\,094\,3(23) \times 10^{-4}$ u from the 2006 CODATA compilation of fundamental constants [15]. The mass of $^{28}Si^{13+}$ is calculated from the atomic mass $M(^{28}\mathrm{Si}) = 27.976\,926\,535\,0(6)$ u, measured by Redshaw, McDaniel, and Myers [16], corrected by the masses of 13 electrons and their respective binding energies, taken from Ref. [17]. The uncertainty of these values contributes to 2.6×10^{-11} to the ion total mass. We arrive at $M(^{28}Si^{13+}) = 27.969\,800\,594\,9(7)$ u. Our final experimental result for the g factor is $g = 1.995\,348\,958\,7(5)(3)(8)$. The first number in brackets is the statistical and the second one the systematical uncertainty, and the third one represents the uncertainty of the electron mass.

In order to match the accuracy of the experiment, various contributions have to be taken into account in theoretical calculations. The dominant terms such as relativistic binding, one-loop QED self-energy, and recoil corrections due to the finite mass of the nucleus have been sufficiently tested in earlier experiments. Besides these, at $Z = 14$, the corrections due to the finite nuclear radius, higher-order vacuum polarization effects, and two-loop QED contributions gain importance. Table I summarizes the theoretical predictions for the $^{28}Si^{13+}$ ion. We have found that even if the ^{28}Si nucleus is quadrupole deformed, terms due to the nuclear deformation (which cannot be described by a spherically averaged root-mean-square radius) are negligible in the present case. Furthermore, the nuclear electric polarizability and magnetic susceptibility corrections are also not visible in the current experiment.

In this experiment, two-loop bound-state QED corrections have become relevant for the first time. In previous measurements with C [2] and O [3], the two-loop QED effects were contributing only at the order $(Z\alpha)^0$, i.e., in the free-electron approximation. In the current case, the correction of order $(Z\alpha)^2$ is clearly visible and the contribution of order $(Z\alpha)^4$ is comparable to the experimental uncertainty. The so far unknown two-loop QED correction of even higher orders in $Z\alpha$ may be extracted from the experimental value by using the tabulated nuclear radius $\langle r^2\rangle_{\mathrm{tab}}^{1/2}(^{28}\mathrm{Si}) = 3.1223(24)$ fm from Ref. [18] in the finite nuclear size correction. Doing so we arrive at $g_{2L}^{(\mathrm{ho})}(Z = 14) = 0.7(1.1) \times 10^{-9}$. Furthermore, the higher-order vacuum polarization terms have been tested for the first time.

TABLE I. Values of individual contributions to the g factor. Abbreviations are as follows: "h.o.," a higher-order contribution; "SE," the self-energy correction; "VP-EL," the electric-loop vacuum polarization correction; "VP-ML," the magnetic-loop vacuum polarization correction; "rad-rec," the leading term of the mixed radiative-recoil correction. The value of the recoil correction of m/M order was interpolated from the results of Ref. [5], and the given uncertainty corresponds to the interpolation.

			Ref.
$\langle r^2\rangle^{1/2}$ [fm]		3.1223(24)	[18]
Dirac value		1.993 023 571 6	
Finite nuclear size		0.000 000 020 5	
One-loop QED	$(Z\alpha)^0$	0.002 322 819 5	
	$(Z\alpha)^2$	0.000 004 040 7	[19]
	$(Z\alpha)^4$	0.000 001 244 6	[4]
	h.o. SE	0.000 000 542 8(3)	[20]
	h.o. VP-EL	0.000 000 032 6	[6]
	h.o. VP-ML	0.000 000 002 5	[21]
$\geq$ Two-loop QED	$(Z\alpha)^0$	−0.000 003 515 1	[15]
	$(Z\alpha)^2$	−0.000 000 006 1	[19]
	$(Z\alpha)^4$	−0.000 000 001 3	[22]
	h.o.	0.000 000 000 0(17)	[22]
Recoil	m/M	0.000 000 206 1(1)	[5]
	rad-rec	−0.000 000 000 2	[6]
	h.o.	−0.000 000 000 1	[23]
Total		1.995 348 958 0(17)	

Vice versa, it is also possible to determine the nuclear charge radius of the isotope ^{28}Si by means of a comparison between the experimental and the theoretical values of the g factor [24]. Looking for the root-mean-square radius $\langle r^2\rangle^{1/2}$ that satisfies the equation $g_{\mathrm{exp}} = g_{\mathrm{th}}(\langle r^2\rangle^{1/2})$, we arrive at the result $\langle r^2\rangle^{1/2}(^{28}\mathrm{Si}) = 3.18(15)$ fm, which is in good agreement with the literature value [18] given above. Although the extracted value is not competitive with the established one, our current proof-of-principle experiment demonstrates the feasibility of this method of nuclear radius determination. This procedure also calls for calculations of the two-loop higher-order QED correction as it is the main source of the nuclear radius uncertainty in the present range of charge numbers.

In summary, the bound electron g factor of hydrogenlike $^{28}\mathrm{Si}^{13+}$ has been experimentally determined to 5×10^{-10} fractional uncertainty. This is the most precise value of the g factor of a bound electron. The accuracy is limited mainly by the uncertainty of the electron mass. Theoretical bound-state QED calculations including two-loop corrections of orders $(Z\alpha)^2$ and $(Z\alpha)^4$ as well as nuclear size and nuclear recoil corrections result in a value of about 1×10^{-9} uncertainty. The excellent agreement between experimental and theoretical value represents to date the most accurate test of bound-state QED calculations in strong fields. So far uncalculated values of higher-order two-loop contributions become visible for the first time. As a consistency check we determined the nuclear root-mean-square radius of ^{28}Si from the comparison of experimental and theoretical g factors and found agreement to tabulated values within our limits of error.

We acknowledge fruitful discussions with K. Pachucki and V. M. Shabaev. This work was supported by the Max-Planck Society and the Helmholtz Alliance HA216/EMMI.

[1] D. Hanneke, S. Fogwell, and G. Gabrielse, Phys. Rev. Lett. **100**, 120801 (2008).
[2] H. Häffner, T. Beier, N. Hermanspahn, H.-J. Kluge, W. Quint, S. Stahl, J. Verdú, and G. Werth, Phys. Rev. Lett. **85**, 5308 (2000).
[3] J. Verdú, S. Djekić, H. Häffner, S. Stahl, T. Valenzuela, M. Vogel, G. Werth, H.-J. Kluge, and W. Quint, Phys. Rev. Lett. **92**, 093002 (2004).
[4] K. Pachucki, U. D. Jentschura, and V. A. Yerokhin, Phys. Rev. Lett. **93**, 150401 (2004).
[5] V. M. Shabaev and V. A. Yerokhin, Phys. Rev. Lett. **88**, 091801 (2002).
[6] T. Beier, Phys. Rep. **339**, 79 (2000).
[7] S. Sturm, K. Blaum, B. Schabinger, A. Wagner, W. Quint, and G. Werth, J. Phys. B **43**, 074016 (2010).
[8] K. Blaum *et al.*, J. Phys. B **42**, 154021 (2009).
[9] G. Werth, H. Häffner, and W. Quint, Adv. At. Mol. Opt. Phys. **48**, 191 (2002).
[10] A. Wagner, S. Sturm, B. Schabinger, K. Blaum, and W. Quint, Rev. Sci. Instrum. **81**, 064706 (2010).
[11] B. Schabinger, S. Sturm, K. Blaum, W. Quint, A. Wagner, and G. Werth, J. Phys. Conf. Ser. **163**, 012108 (2009).
[12] L. S. Brown and G. Gabrielse, Phys. Rev. A **25**, 2423 (1982).
[13] R. S. Van Dyck, Jr., F. L. Moore, D. L. Farnham, and P. B. Schwinberg, Phys. Rev. A **40**, 6308 (1989).
[14] J. V. Porto, Phys. Rev. A **64**, 023403 (2001).
[15] P. J. Mohr, B. N. Taylor, and D. B. Newell, Rev. Mod. Phys. **80**, 633 (2008).
[16] M. Redshaw, J. McDaniel, and E. G. Myers, Phys. Rev. Lett. **100**, 093002 (2008).
[17] W. Martin and R. Zalubas, J. Phys. Chem. Ref. Data **12**, 323 (1983).
[18] I. Angeli, At. Data Nucl. Data Tables **87**, 185 (2004).
[19] H. Grotch, Phys. Rev. Lett. **24**, 39 (1970).
[20] V. A. Yerokhin, P. Indelicato, and V. M. Shabaev, Phys. Rev. A **69**, 052503 (2004).
[21] R. N. Lee, A. I. Milstein, I. S. Terekhov, and S. G. Karshenboim, Phys. Rev. A **71**, 052501 (2005).
[22] K. Pachucki, A. Czarnecki, U. D. Jentschura, and V. A. Yerokhin, Phys. Rev. A **72**, 022108 (2005).
[23] K. Pachucki, Phys. Rev. A **78**, 012504 (2008).
[24] T. Beier, H. Häffner, N. Hermanspahn, S. Djekic, H. Kluge, W. Quint, S. Stahl, T. Valenzuela, J. Verdú, and G. Werth, Eur. Phys. J. A **15**, 41 (2002).